Influence of the Precursor Cross-Linking Route on the Thermal Stability of Si−B−C−O Ceramics

Vladislav Ischenko,[†] Eckhard Pippel,[†] Jörg Woltersdorf,[†] B. Rodrigue Ngoumeni Yappi,[‡] Ralf Hauser,[‡] Claudia Fasel,[‡] Ralf Riedel,*[,‡] Fabrizia Poli,[§] and Klaus Müller[§]

Max-Planck-Institut für Mikrostrukturphysik, Weinberg 2, D-06120 Halle, Germany, Institut für Materialwissenschaft, Technische Universität Darmstadt, Petersenstrasse 23, D-64287 Darmstadt, Germany, and Institut für Physikalische Chemie, Universität Stuttgart, Pfaffenwaldring 55, D-70569 Stuttgart, Germany

Received July 19, 2007. Revised Manuscript Received September 22, 2008

The specifics of the cross-linking route of tris(1-(dichloro(methyl)silyl)ethyl)borane to form a preceramic polymer suitable for the subsequent synthesis of Si−B−C−O ceramics has significant influence on the local phase composition and the microstructural features of the resulting samples after their ceramization and subsequent annealing. Cross-linking of tris(1-(dichloro(methyl)silyl)ethyl)borane via *hydrolysis* used for the preceramic polymer synthesis increases the amount of nanocrystalline SiC in the resulting Si−B−C−O ceramics up to 1400 °C, while cross-linking with *polyvalent alcohols* allows the homogeneous component distribution to be preserved and the formation of crystalline phases to be retarded. The different contents of bound oxygen in the preceramic polymers, depending on the cross-linking route, may explain the observed different stabilities of amorphous Si−B−C−O against phase separation and crystallization.

1. Introduction

Recently, silicon oxycarbide (Si−C−O) ceramics have gained growing scientific and technological interest due to their enhanced thermal properties compared to pure silica. They are characterized by (i) retaining their amorphous structure up to ultrahigh temperatures, far above temperatures where their binary constituents, namely silica or silicon carbide, transform from the amorphous to the crystalline state;[1] (ii) exhibiting essentially zero steady state creep at very high temperatures (near 1400 °C); creep experiments on silicon oxycarbide glasses showed an increase of the viscosity at temperatures above 1200 °C due to the precipitation of β-SiC, making steady state creep impossible under this condition; thus, their creep resistance is much higher than that of polycrystalline materials of equivalent compositions;[2,3] and (iii) containing excess carbon relative to the stoichiometric mixtures of SiC and SiO_2 but having extremely high oxidation resistance, at the same time.[4]

These unusual properties are obtained exclusively by cross-linking of silicon-containing molecular precursors forming a preceramic polymer followed by pyrolysis of the polymer under controlled conditions. The pyrolysis of preceramic polymers is an alternative method to the classical powder processing routes, which are well used in the manufacturing of a variety of oxide and nonoxide ceramics.[5] Carbon can be easily incorporated in the SiO_2-network by pyrolysis of organopolysiloxanes, which cannot be achieved by traditional solid state reaction of silica with carbon.

While the first Si−C−O fibers could be obtained through partial hydrolysis and oxidation of polycarbosilane fibers,[6,7] the first silicon oxycarbide ceramic was obtained after pyrolysis of polysiloxane synthesized by a sol−gel method. Silicon oxycarbide glasses have found several high-temperature applications as compared with pure SiO_2 glasses, for example, as catalyst supports and fiber coatings.[8−10]

The influence of the chemical composition and molecular structure of the preceramic polymer on the properties of the obtained ceramic has yet to be understood. While numerous publications dealt with the incorporation of boron in polysilazanes to increase their thermochemical stability after pyrolysis, only few papers reported on boron-containing polysiloxanes.[11−19] It was shown that the presence of boron in Si−C−O ceramics leads to enhanced crystallization of

* Corresponding author. E-mail: riedel@materials.tu-darmstadt.de.
[†] Max-Planck-Institut für Mikrostrukturphysik.
[‡] Technische Universität Darmstadt.
[§] Universität Stuttgart.

(1) Scarmi, A.; Soraru, G. D.; Raj, R. *J. Non-Cryst. Solids* **2005**, *351* (27−29), 2238–2243.
(2) Jia, N. Y.; Bodet, R.; Tressler, R. E. *J. Am. Ceram. Soc.* **1993**, *76* (12), 3051–3060.
(3) Rouxel, T.; Soraru, G. D.; Vicens, J. *J. Am. Ceram. Soc.* **2001**, *84* (5), 1052–1058.
(4) Raj, R.; Riedel, R.; Soraru, G. D. *J. Am. Ceram. Soc.* **2001**, *84* (10), 2158–2159.
(5) Riedel, R. In *Materials Science and Technology*; Advanced Ceramics from Inorganic Polymers; Cahn, R. W., Haasen, P., Kramer, E. J., Brook, R. J., Eds.; Wiley-VCH: Weinheim, 1996; Volume *17B*, pp 1−50.
(6) Yajima, S.; Hayashi, J.; Omori, M. *Chem. Lett.* **1975**, (9), 931–934.
(7) Lipowitz, J.; Freeman, H. A.; Chen, R. T.; Prack, E. R. *Adv. Ceram. Mater.* **1987**, *2* (2), 121–128.
(8) Babonneau, F; Thorne, K; Mackenzie, J. D. *Chem. Mater.* **1989**, (1), 554–558.
(9) Renlund, G. M.; Prochazka, S.; Doremus, R. H. *J. Mater. Res.* **1991**, *6* (12), 2716–2722.
(10) Soraru, G. D.; Dallapiccola, E.; DAndrea, G. *J. Am. Ceram. Soc.* **1996**, *79* (8), 2074–2080.
(11) Pantano, C. G.; Singh, A. K.; Zhang, H. X. *J. Sol-Gel Sci. Technol.* **1999**, *14* (1), 7–25.
(12) Riedel, R.; Bill, J.; Kienzle, A. *Appl. Organomet. Chem.* **1996**, *10* (3−4), 241–256.
(13) Riedel, R.; Kienzle, A.; Dressler, W.; Ruwisch, L.; Bill, J.; Aldinger, F. *Nature* **1996**, *382* (6594), 796–798.

10.1021/cm701916g CCC: $40.75
Published on Web 11/01/2008

β-SiC and inhibits the formation of crystalline SiO_2.[20] Thus, the matrix and surface cracking associated with the phase transformation of cristobalite during cooling and heating, which could deteriorate the mechanical strength, can be avoided.[21] Furthermore, Raman measurements confirmed the inhibition of the separation of free carbon in boron containing materials up to 1400 °C providing a higher electrical resistivity as compared to boron free Si−C−O.[22] Thus, it can be stated from the results published in the literature that the incorporation of boron generally enhances the thermal stability of silicon oxycarbide ceramics at least up to 1400 °C. The Si−B−C−O system could be therefore an excellent candidate material for high temperature applications, including fibers for ceramic matrix composites (CMCs). At 1500 °C and higher, boron was found to enhance the growth of segregated sp^2-carbon nanocrystals.[23]

Here we report on the thermal stability against crystallization and phase partitioning of three different Si−B−C−O ceramic compositions. In particular the influence of the precursor cross-linking route on the thermal behavior was studied. The boron-containing polysiloxanes were synthesized by hydrolysis and alcoholysis of a ((chloro(methyl)-silyl)ethyl)borane as the starting molecule followed by cross-linking via polycondensation.

2. Experimental Section

2.1. Synthesis and Characterization of the Polymer Precursors. All reactions described below were carried out in argon atmosphere using Schlenk techniques.[24] Dichloromethylvinylsilane and borane dimethylsulfide were obtained from Aldrich (Milwaukee, U.S.A.) and used without further purification. The synthesis of the three polymer series was done in two steps: (i) synthesis of tris(1-(dichloro(methyl)silyl)ethyl)borane monomer and (ii) subsequent polymerization of the monomer by means of three different cross-linking routes.[25]

2.1.1. Synthesis of Tris(1-(dichloro(methyl)silyl)ethyl)borane, Monomer B. The boron-containing monomer B was prepared according to the following hydroboration reaction route (eq 1): 100 mL (108.5 g, 0.76 mol) of commercially available dichloromethylvinylsilane was put in a 1 L Schlenk flask equipped with a magnetic stir bar, solved in toluene, and cooled at 0 °C. After stirring for 30 min, 23.6 mL (19 g, 0.25 mol) of borane dimethylsulfide was added dropwise and stirred at room temperature for 30 h to obtain 107 g (98%) of tris(1-(dichloro(methyl)silyl)ethyl)borane B after the solvent has been removed by distillation under reduced pressure at 40 °C.

Table 1. Amount of Reactants and Product Yield in the Polymerization Reactions of Tris(1-(dichloro(methyl)silyl)ethyl)borane

sample	amount of monomer B	cross-linking agent	amount of cross-linking agent	yield of the polymer
H series	10 mL (0.029 mol)	water	3.07 mL (0.174 mol)	4.62 g (85%)
A1 series	10 mL (0.029 mol)	glycerine	4.16 mL (0.057 mol)	8.94 g (78%)
A2 series	10 mL (0.029 mol)	glycol	4.75 mL (0.085 mol)	10.26 g (88%)

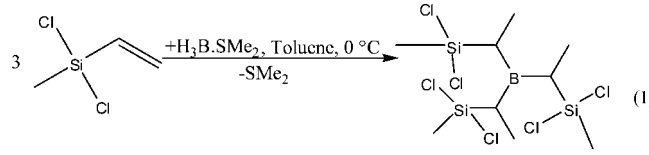

In reaction 1 hydroboration of the vinylsilane in the α-position is shown exclusively for simplification. Previous studies have shown that also hydroboration in β-position occurs, which is not again discussed here. Details of the hydroboration reaction of dichloromethylvinylsilane with borane dimethylsulfide have been published by Kienzle[25] and by Ruwisch et al.[26]

2.1.2. Polymerization of Tris(1-(dichloro(methyl)silyl)ethyl)-borane. To obtain the polymer precursors for H, A1, and A2 series (reaction schemes 2, 3, and 4, respectively), 10 mL (0.029 mol) of monomer B was put in a flask, solved in tetrahydrofuran (THF), and cooled at 0 °C. After stirring for 10 min, the stoichiometric amount of the cross-linking agent (see Table 1) solved in THF was added slowly and subsequently refluxed at 72 °C for 2 h. After cooling, the solvent was removed under reduced pressure, and a white solid polymer was isolated.

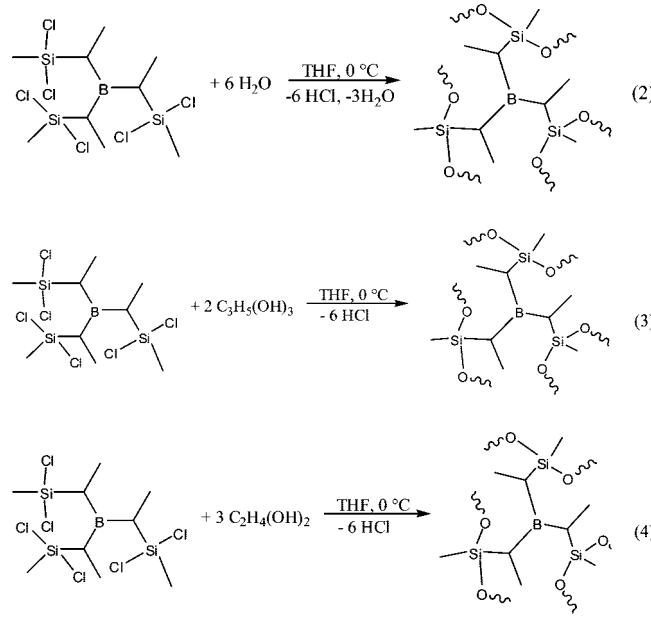

The elemental composition of the polymers in terms of Si, B, C, O, and Cl content was analyzed by Mikrolabor Pascher, Remagen, Germany. The analysis data are summarized in Table 2.

2.2. Pyrolysis of the Polymers and Spectroscopic and Thermal Analyses. The samples pyrolyzed at 1400 °C under thermal analysis conditions (see section 2.2.2) have been used for

(14) Baldus, H. P.; Jansen, M. *Angew. Chem., Int. Ed. Engl.* **1997**, *36* (4), 329–343.
(15) Weinmann, M.; Schuhmacher, J.; Kummer, H.; Prinz, S.; Peng, J. Q.; Seifert, H. J.; Christ, M.; Muller, K.; Bill, J.; Aldinger, F. *Chem. Mater.* **2000**, *12* (3), 623–632.
(16) Jansen, M.; Jaschke, B.; Jaschke, T. *High Perform. Non-Oxide Ceram. I* **2002**, *101*, 137–191.
(17) Wootton, A. M.; Rappensberger, M.; Lewis, M. H.; Kitchin, S.; Howes, A. P.; Dupree, R. *J. Non-Cryst. Solids* **1996**, *204* (3), 217–227.
(18) Soraru, G. D.; Campostrini, R.; Maurina, S.; Babonneau, F. *J. Am. Ceram. Soc.* **1997**, *80* (4), 999–1004.
(19) Soraru, G. D.; Babonneau, F.; Maurina, S.; Vicens, J. *J. Non-Cryst. Solids* **1998**, *224* (2), 173–183.
(20) Schiavon, M. A.; Gervais, C.; Babonneau, F.; Soraru, G. D. *J. Am. Ceram. Soc.* **2004**, *87* (2), 203–208.
(21) Liebau, V.; Hauser, R.; Riedel, R. *C. R. Chim.* **2004**, *7* (5), 463–469.
(22) Klonczynski, A.; Schneider, G.; Riedel, R.; Theissmann, R. *Adv. Eng. Mater.* **2004**, *6* (1−2), 64–68.
(23) Peña-Alonso, R.; Mariotto, G.; Gervais, C.; Babonneau, F.; Soraru, G. D. *Chem. Mater.* **2007**, *19* (23), 5694–5702.
(24) Shriver, D. F.; Drezdon, M. A. *The Manipulation of Air-Sensitive Compounds*; Wiley: New York, 1986; Vol. 2.
(25) Kienzle, A., Ph.D. Thesis, University of Stuttgart, Stuttgart, Germany, 1994.
(26) Ruwisch, L. M.; Dürichen, P.; Riedel, R. *Polyhedron* **2000**, *19*, 323–330.

Table 2. Elemental Analysis of the As-Synthesized Preceramic Polymers and of the Ceramics Obtained Therefrom at 1400 °C after Pyrolysis under Argon

	element content of the polymers[a] (wt %)					composition of the polymers (expected)
	Si	B	C	Cl	O	
H series	27.7	3.4	40.4	3.1	18.5	$Si_{3.1}B_{1.0}C_{10.7}O_{3.7}Cl_{0.3}$ ($Si_3B_1C_9H_{21}O_3$)
A1 series	17.9	2.4	43.3	3.6	26.2	$Si_{2.9}B_{1.0}C_{16.4}O_{7.5}Cl_{0.5}$ ($Si_3B_1C_{15}H_{31}O_6$)
A2 series	19.4	2.5	41.1	1.2	26.8	$Si_{3.0}B_{1.0}C_{14.9}O_{7.3}Cl_{0.2}$ ($Si_3B_1C_{15}H_{33}O_6$)
	element content of the resulting ceramics (wt %)					composition of the resulting ceramics
	Si	B	C	Cl	O	
H series	40.30	4.35	32.40	<0.50	21.90	$Si_{3.0}B_{0.8}C_{5.6}O_{2.9}(Cl_{<0.03})$
A1 series	39.20	3.15	17.80	0.66	37.98	$Si_{3.0}B_{0.6}C_{3.2}O_{5.1}(Cl_{0.04})$
A2 series	41.30	0.83	30.76	0.57	24.68	$Si_{3.0}B_{0.2}C_{5.2}O_{3.1}(Cl_{0.03})$

[a] The amount of hydrogen has not been analyzed and is assumed to balance to 100%, namely, 6.9 wt % for the H-polymer, 6.6 wt % for the A1-polymer, and 9.0 wt % for the A2-polymer.

the comparative study along with the samples pyrolyzed in a quartz tube under continuous argon flow at 1100 °C with a heating rate of 100 °C h^{-1}. In the latter case, the dwelling time at the final temperature was 3 h. The furnace was then automatically turned off, and the samples were cooled down to room temperature.

2.2.1. NMR and IR Spectroscopy. The polymers were investigated using NMR and Fourier transform infrared (FT-IR) spectroscopy. NMR spectra were recorded on a Bruker DRX 500 spectrometer (99.4 MHz for ^{29}Si; 160.5 MHz for ^{11}B) using THF-d_8 as solvent. Shifts are given relative to external tetramethylsilane (^{29}Si) and borontrifluoride diethyletherate (^{11}B).

The Si−B−C−O ceramics were analyzed by solid state ^{11}B-MAS NMR spectroscopy using a Bruker CXP 300 spectrometer, operating at a static magnetic field of 7.05 (^{1}B frequency: 96.29 MHz). The measurements were run using a 4 mm magic angle spinning (MAS) probe, with a rotation frequency of 14 kHz. All ^{11}B NMR spectra were recorded using single pulse excitation and a recycle delay of 10 s. The number of scans ranged from 500 to 2000 depending on the sample. The ^{11}B chemical shifts were determined relative to a solution of boric acid as secondary standard ($\delta = 18.89$ ppm with respect to the primary standard, $(OEt)_2BF_3$, at $\delta = 0$ ppm).

FT-IR spectra were recorded on a Perkin-Elmer FT-IR 1750 using a diamond single reflection ATR unit from Specac Inc. (U.K.).

2.2.2. Thermal and Chemical Analyses. Quantitative thermal analyses studies of the polymer and of the formed ceramics were performed with a simultaneous thermal analyzer STA 429 (Netzsch, Germany). For these measurements, the samples were heated under an argon flow up to 1400 °C with a heating rate of 5 °C min^{-1}. The gases evolved during pyrolysis were detected with a Balzers QMA 400 mass spectrometer coupled to the STA equipment.

The Si, B, and Cl contents of the ceramics were analyzed by Mikrolabor Pascher, Remagen, Germany. The elemental analyses data (Pascher) were obtained by repeat determination. The O and C content of the ceramics were measured by hot gas extraction using an N,O-Analyzer Leco TC-436 and by combusion analysis with a C-Analyzer Leco C-200, respectively. The standard deviation is below 1% in all cases.

2.3. Microstructural and Nanochemical Analyses of the Ceramic Products. The local phase composition and the microstructural features of the fragmented Si−B−C−O ceramics after thermal treatment at 1100 and 1400 °C were investigated by high resolution transmission electron microscopy (HRTEM), scanning electron microscopy (SEM), and electron energy-loss spectroscopy (EELS), especially of the near-edge fine structures (ELNES). The HREM and EELS investigations were carried out in a combined scanning/transmission electron microscope (TEM/STEM, CM 20 FEG, Philips, Eindhoven, The Netherlands) having a point resolution of 0.24 nm and an operating voltage of 200 kV, equipped with a postcolumn electron energy filter (Gatan Imaging Filter GIF 200, model 667, Pleasanton, CA) as well as with a digital scanning module (Gatan Digiscan). In addition, the surface morphology of the bulk phase was characterized by SEM, using a JEOL 6300F instrument, operating at 5.0 kV. EELS was performed with an energy resolution of about 0.8 eV. Point analyses were made in the nanoprobe mode with the electron probe of a few nanometers in diameter. For spectrum processing, the software packages Digital Micrograph and EL/P of Gatan were used.

3. Results and Discussion

3.1. Preceramic Polymers and Their Ceramization to SiBCO Ceramic. Cross-linking of tris(1-(dichloro(methyl)-silyl)ethyl)borane with water (H series) or polyvalent alcohols (A1 and A2 series) resulted in Si−B−C−O polymers, suitable for the subsequent ceramization at higher temperatures. IR and NMR spectroscopy confirmed the expected molecular structure of the polymers: FT-IR studies revealed absorption bands that can be assigned to the presence of B−C (1100 cm^{-1}) as well as Si−CH_3 bonds (1250 cm^{-1}) in the three polymer series (H, A1, and A2). Absorption bands, which could be related to Si−O−C and Si−O−Si groups, were measured between 1000 cm^{-1} and 1100 cm^{-1} for the alcoholized and hydrolyzed samples. Chemical analysis data (see Table 2) are in the range of the calculated compositions. It can be also taken from Table 2 that the synthesized polymer samples still contain some residual chlorine contamination.

^{29}Si NMR spectra of the polymers H, A1, and A2 showed broad signals in the range between $\delta = -6$ and -22 ppm, indicating the presence of cyclic siloxane units.[27] Thus, it is assumed that the synthesized Si polymers are constituted of cyclic siloxane units interconnected via C−B−C bridges. In sample A2, additional chemical shift values between $\delta = +4$ and $+17$ ppm are assigned to nonalcoholyzed residual Si−Cl end-groups of the polymer.[24,28−30] In the ^{11}B-NMR spectrum of all three samples a single chemical shift value

(27) Horn, H. G.; Marsmann, H. C. *Makromol. Chem.* **1972**, *162*, 255.
(28) Ruwisch, L. *Synthese und Hochtemperaturverhalten borhaltiger Siliciumcarbonitride*; Shaker-Verlag: Aachen, Germany, 1998.
(29) Schramml, J.; Chvalovsky, V.; Mägi, M.; Lippmaa, E. *Collect. Czech. Chem. Commun.* **1979**, *44*, 854.

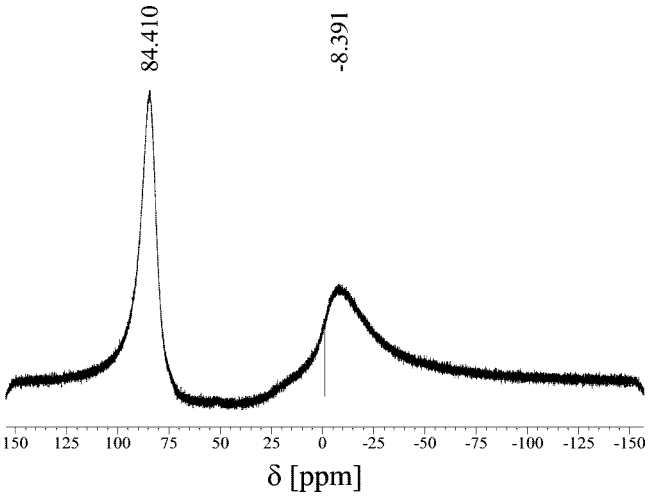

Figure 1. ^{11}B-NMR spectrum of polymer H. The chemical shift $\delta = -8.4$ ppm is assigned to the borosilicate glass of the NMR tube used for the measurement.

located at $\delta = +84$ ppm was detected indicating the presence of trigonally planar coordinated BC_3 units as shown for sample H in Figure 1.

The thermal decomposition behavior of the Si−B−C−O polymers was studied between room temperature and 1400 °C by thermal gravimetric analysis (TGA) as well as by in situ mass spectrometry during the pyrolysis process as presented in Figure 2. The TGA curves basically exhibit one major weight loss step (Figure 2a−c) for all three samples between 200 and 400 °C. The overall weight loss of the A1 and A2 series is significantly higher compared to that of sample H, and the obtained ceramic yields of compounds A1, A2, and H amount to 20, 25, and 65 wt %, respectively (Figure 2a−c).

In situ mass spectrometric analysis revealed the loss of $C_xH_yO_z$ fragments for the samples A1 and A2 in the temperature range between room temperature and 200 °C (not shown in Figure 2). The main fragments analyzed correspond to the following *m*/*z* values with the respective assignments given in brackets: for sample A1, $m/z = 27$ ($C_2H_3^+$), 42 ($C_3H_6^+$ or $C_2H_2O^+$), 43 ($C_3H_7^+$ or $C_2H_3O^+$), and 57 (C_4H_9+ or $C_3H_5O^+$); for sample A2, $m/z = 43$ ($C_3H_7^+$ or $C_2H_3O^+$) and 73 ($C_4H_9O^+$ or $C_3H_5O_2^+$).

The loss of $C_xH_yO_z$ species clearly indicates the decomposition of the O−CH_2−CH_2−O− and O−CH_2−CH(O)−CH_2−O bridging units present in the A1 and A2 polymer series and formed by the cross-linking reaction of the hydroborated chlorosilane B with glycerine and glycol, respectively. In case of polymer H we could not detect any similar outgassing species in the same temperature range.

The observed mass decrease between 300 and 450 °C is related to the loss of the hydrocarbon $C_2H_4^+$ ($m/z = 28$) as shown in Figure 2a while hydrogen with $m/z = 2$ and methane identified by $m/z = 15$ (CH_3^+) are evolved between 300 and 700 °C and 400 and 700 °C, respectively (Figure 2a). In the case of polymer A1, the temperature dependent release of H_2 shows one broad peak between 400 and 700 °C (Figure 2b) while sample A2 exhibits two maxima at 200−400 °C and 500−700 °C (Figure 2c). It is obvious that, in all samples, the loss of hydrogen is always found along with the outgassing of hydrocarbons.

Despite the similar thermal behavior of the three different polymers during pyrolysis, compounds A1 and A2 exhibit a pronounced mass decrease up to 500 °C, which is due to the supplementary release of further hydrocarbons. This finding is supported by the presence of propene, identified by the fragment $[C_3H_5]^+$ with $m/z = 41$ (not shown in Figure 2), as detected by mass spectrometry. In contrast, sample H did not show the appearance of mass $m/z = 41$ over the whole temperature range. It is worth mentioning that the masses $m/z = 27$ and $m/z = 28$ were detected for all three samples due to the evolution of C_2H_4 (Figure 2). The appearance of the mass $m/z = 27$ at the same temperature as $m/z = 28$ clearly excludes the possible formation of CO with the same mass $m/z = 28$. Even at higher temperatures, no evolution of CO was observed for the three samples, indicating that no carbothermal reaction occurred in the investigated temperature range between 1000 and 1400 °C. This finding is an important result since the decomposition of Si−O−C ceramics was reported earlier in some cases due to the carbothermal reaction with the simultaneous formation of CO and SiC.[31]

In addition, signals related to higher masses like $m/z = 61$, $m/z = 70$ (Figure 2d), and $m/z = 103$ are analyzed for sample A2 which can be assigned to $C_2H_5O_2^+$, $C_4H_6O^+$ or $C_5H_{10}^+$, and $C_8H_7^+$, respectively. This result of further evolution of $C_xH_yO_z$ fragments is confirmed by the fact that in the same temperature range, the mass $m/z = 12$ for C^+ is found indicating hydrocarbon based molecules as the outgassing species. The thermal decomposition of the polymers H, A1, and A2 is completed mostly at around 800 °C. No further significant mass loss is detected between 800 and 1400 °C for all three samples.

The elemental analysis data of the sample series before and after pyrolysis are listed in Table 2. Accordingly, the molar oxygen content of the three polymer series differs significantly while that of the ceramics is the same for H and A2. The ceramic obtained from polymer A1 contains nearly the double molar amount of oxygen as compared to the H and A2 samples. It can be taken from Table 2 that during thermal decomposition of the Si−B−C−O polymers the initial molar amount of oxygen is reduced by 25, 37.5, and 57% for the H, A1, and A2 series, respectively. This finding has to be explained by the distinct bridging units formed from water, glycerine, and glycol as cross-linking agents (see below). Since no CO, SiO, or boron oxide species could be detected in our TGA-MS studies, the loss of oxygen has to be ascribed to the evolution of oxygen containing hydrocarbons formed during pyrolysis.

At the same time, the samples of the H series show a significantly lower loss of carbon (51%), compared to the samples of the A1 and A2 series (ca. 80% and 65%, respectively). It is interesting that, starting from polymers

(30) Herzog, U.; Notheis, C.; Brendler, E.; Roewer, G. *Fresenius J. Anal. Chem.* **1997**, *357*, 503–504.

(31) Saha, A.; Raj, R. *J. Am. Ceram. Soc.* **2007**, *90* (2), 578–583.

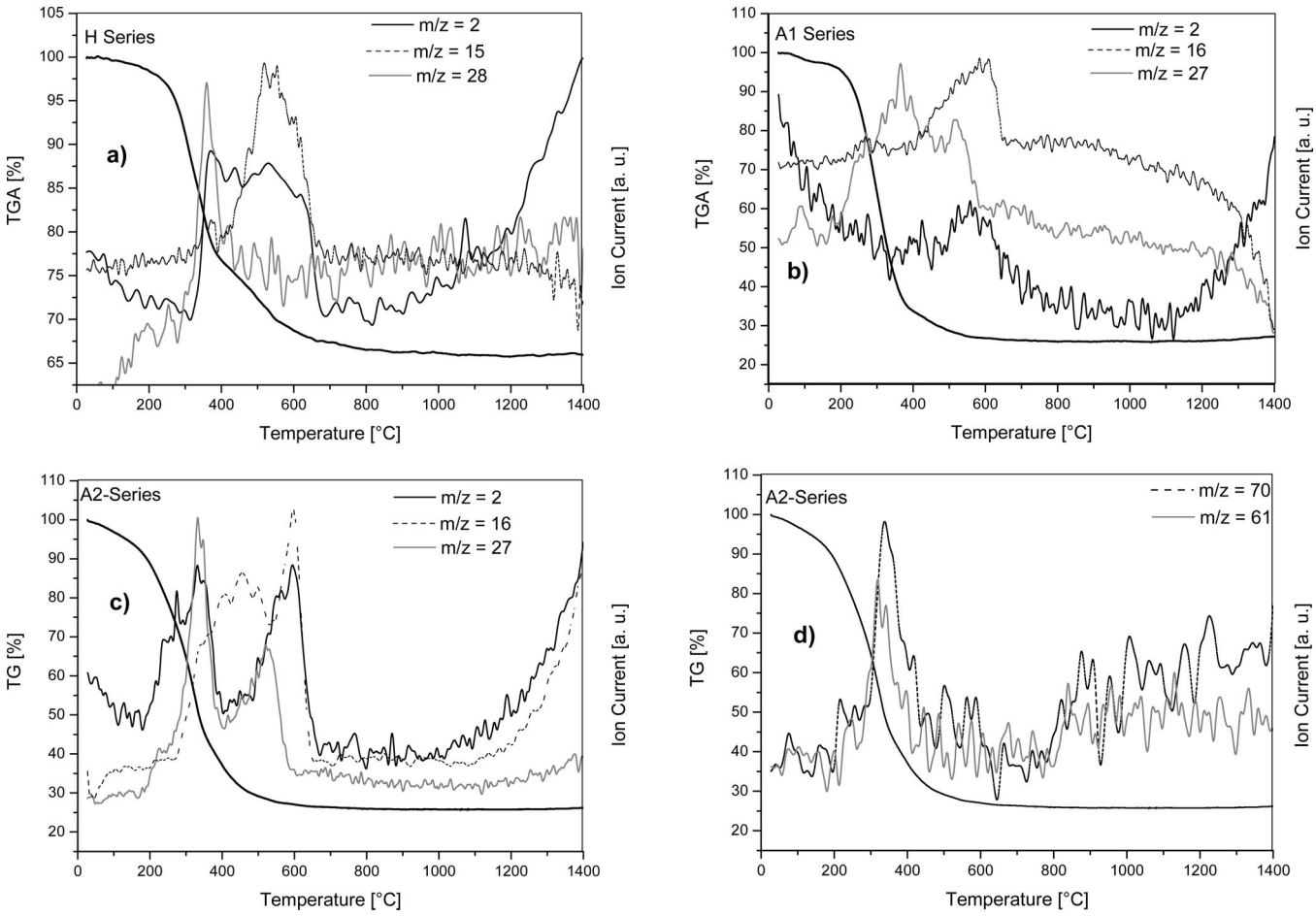

Figure 2. a−d: Thermal gravimetric analysis with in situ mass spectroscopy measurements between room temperature and 1400 °C: (a) H series, (b) A1 series, and (c and d) A2 series.

with a higher molar carbon content in the A series, compared to the H series, the pyrolysis leads to ceramics with comparable or even lower molar carbon contents (Table 2). This phenomenon has to be discussed in the light of the different decomposition reactions involved during polymer-to-ceramic transformation of the individual polymers derived by hydrolysis and alcoholysis of the hydroborated chlorosilane B.

The presence and the local structure of boron atoms in the Si−B−C−O ceramic samples after pyrolysis at 1400 °C were studied by ^{11}B MAS NMR spectroscopy. ^{11}B NMR spectra of the H, A1, and A2 are reported in Figure 3. The ^{11}B NMR spectra of all samples show a characteristic second order quadrupolar broadening for boron atoms in asymmetrical environments. They can be assigned to boron atoms in a trigonal BX_3 configuration, as for example BO_3 in boron oxide B_2O_3. However, the observed overall ^{11}B NMR line shapes depend on the actual sample. Hence, the spectrum of sample A1 is characterized by a pure second order quadrupolar powder pattern, reflecting the presence of a single type of BO_3 unit. Conversely, the line shapes observed for samples H and A2 reflect an overlap of at least two different components, pointing to the presence of BO_3 units in different chemical surroundings. According to a former ^{11}B NMR study on Si−B−C−O glasses prepared by the sol−gel route,[19] these components may be attributed to ^{11}B nuclei with different second coordination spheres, as, for instance, BO_3 trigonal units with =B−O−B= and =B−O−Si= structural elements.

From the solid state ^{11}B NMR results two basic conclusions can be clearly drawn: Firstly, in all three samples, the boron coordination changes from BC_3 sites in the polymeric materials to BO_3 sites in the Si−B−C−O ceramics. Secondly, the line shapes of the NMR signals are different for all three samples indicating different mechanisms associated with the polymer-to-ceramic transformation due to the use of water (H series), glycerine (A1 series), or glycol (A2 series) as cross-linking agent.

3.2. Microstructure and Phase Composition of Si−B−C−O Ceramics. A remarkable effect of the cross-linking method on the morphology of the Si−B−C−O ceramics after annealing at high temperature (1400 °C) has been revealed by SEM: As demonstrated in Figure 4a, the Si−B−C−O matrix contains in the case of the hydrolyzed specimens (H series) a considerable amount of smaller particles of 20−50 nm in size (emerging also on the surface of the larger fragments), which turn out to be crystalline silicon carbid nanoparticles, as shown additionally in Figure 4b. In contrast, the alcoholyzed samples A1 and A2 deliver only pure glassy Si−B−C−O fragments (Figure 4c,d) without additional formation of crystalline nanoparticles.

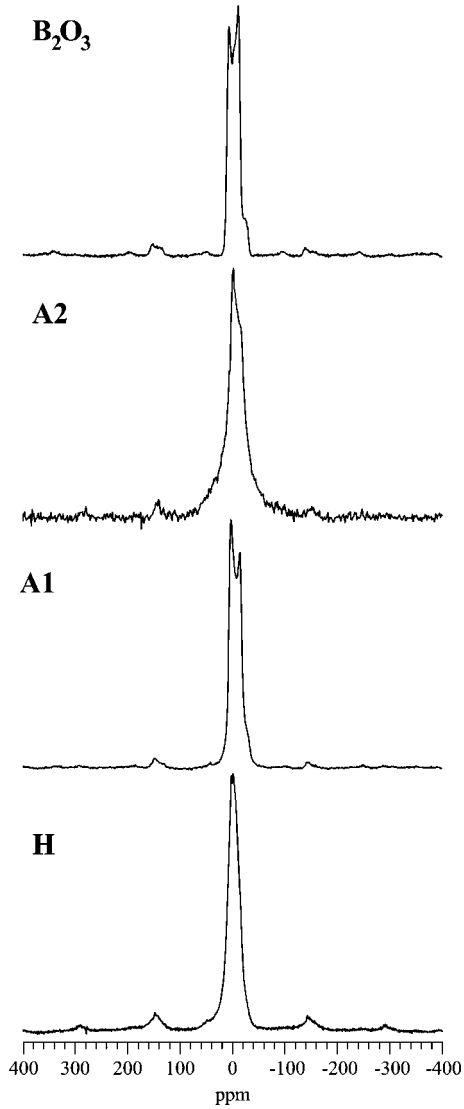

Figure 3. ^{11}B MAS NMR spectra of samples H, A1, and A2 after pyrolysis at 1400 °C under continuous Ar flow. Boron oxide (B_2O_3) is shown for reference.

HRTEM investigations of the different series at the nanoscale revealed the size, the distribution, and the chemical composition of the crystalline regions within the Si−B−C−O matrix: As demonstrated in Figure 5a, the hydrolyzed samples (series H) contain numerous inclusions of nanocrystalline silicon carbide (Figure 6) of some tens of nanometers in size within the glassy matrix, corresponding to the findings at the fragment surfaces, described above. In contrast, the A1 samples (alcoholyzed with glycerine) reveal only few very small inclusions of nanocrystalline SiC (cf. Figure 5b), and the A2 samples (alcoholyzed with glycol) show no SiC particles at all. Thus, the bulk of the ceramic products of the alcoholysis cross-linking routes remain essentially amorphous (Figures 5b,c). Worth mentioning are the inclusions of turbostratic graphite, which were observed in a variable amount in all samples but to a significantly larger extent in the A2 series, as demonstrated in Figure 5c, where the orientation of the graphite basal planes is indicated with guidelines.

EEL spectroscopy revealed that within the H samples, annealed at 1400 °C, the distribution of carbon is strongly

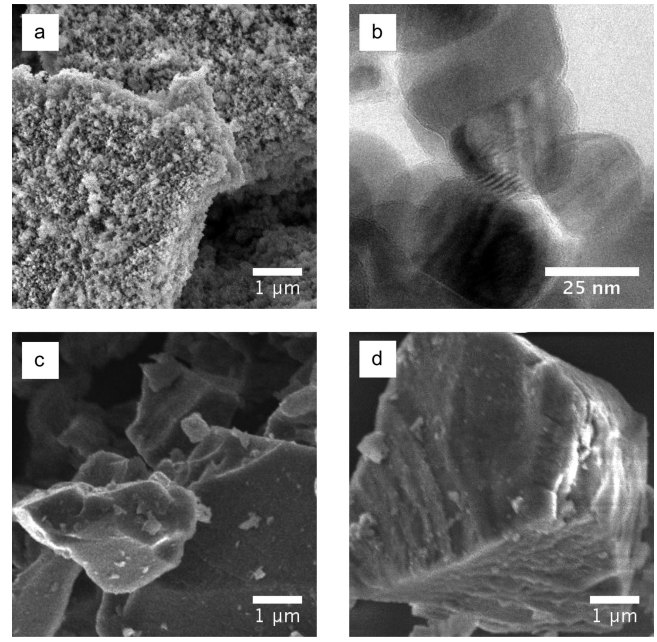

Figure 4. (a, c, d) SEM micrographs of surface morphology of Si−B−C−O fragments heated up to 1400 °C: (a) H series, (b) A1 series, and (c) A2 series. (b) TEM micrograph showing the morphology of the H series sample near the surface of the SiBOC ceramics.

inhomogeneous. For the amorphous regions in this sample, the Si-$L_{2,3}$ edge is quite typical for that usually observed for amorphous SiO_2, while the Si-$L_{2,3}$ edge for the above-mentioned nanocrystalline inclusions is completely consistent with that for crystalline SiC (cf. Figure 6). The intensity of the C−K peak is very small in the amorphous regions, suggesting that they contain very little carbon and should be close to SiO_2 in their composition, while practically all the carbon is concentrated in the crystalline SiC phase.

The segregation of SiC occurs to a much lower extent in the samples obtained by using the *alcoholysis* cross-linking routes A1 and A2: Figure 7 compares the changes in the observed C−K edge in EEL spectra of different samples, which appear with the increase of the annealing temperature from 1100 to 1400 °C. While the samples from all three routes show a similar C−K edge at 1100 °C, at higher temperature the difference becomes remarkable: Along with the above-mentioned decrease of the C−K peak intensity in the amorphous bulk of H samples due to the separation of crystalline SiC, the more clear appearance of the peak at 284 eV in the case of A2 samples (glycol) suggests that carbon becomes partially segregated in the form of graphite in these samples at 1400 °C (Figure 7). The more frequent observation of the oriented graphene sheets in the A2 samples with HRTEM (Figure 5c) supports this quite well. Less pronounced is the segregation of carbon in the A1 samples (glycerine) which is due to the lower carbon content present in this sample as compared to the compositions of A2 and H (Table 2). The fine structure of the Si-$L_{2,3}$ edge provides an additional confirmation of this finding: The first peak for the A1 sample, treated at 1400 °C, exhibits a lower relative intensity and a broader tail toward lower energies, implying an increased amount of carbidic bonding in the nearest coordination sphere of silicon (Figure 8). The O−K edge in the ELNES of the H samples, treated at 1400 °C, shows a

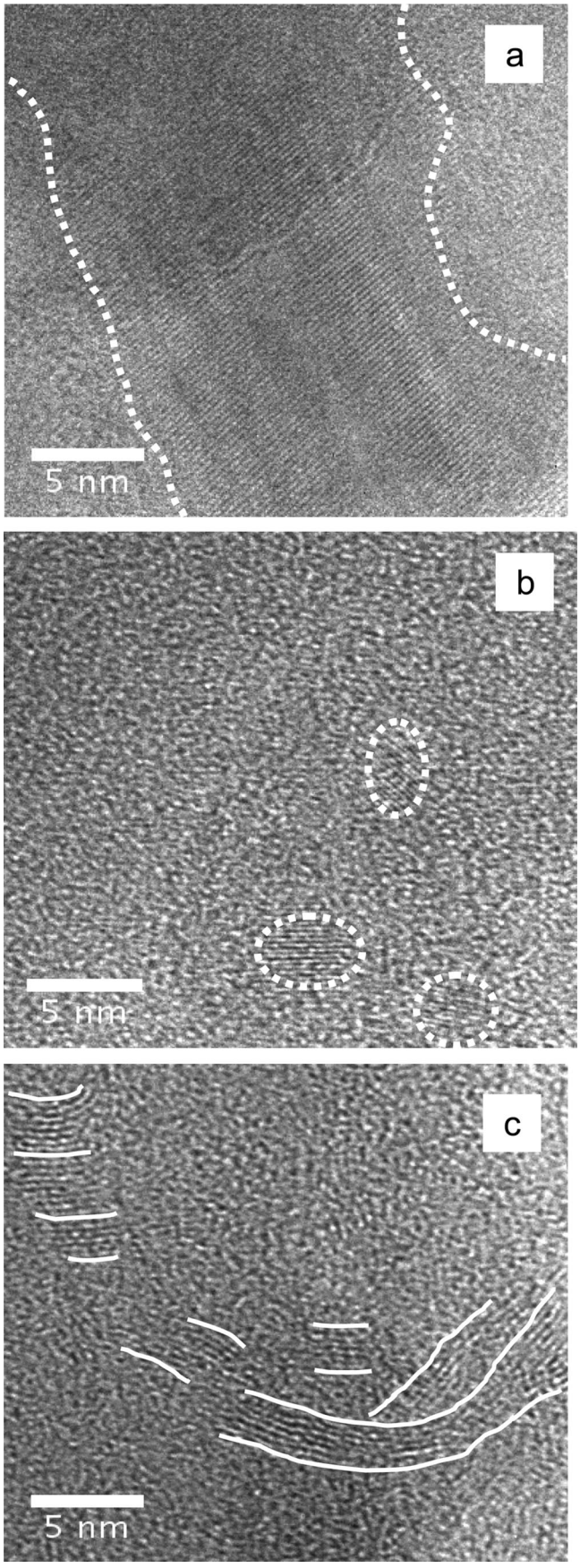

Figure 5. HREM images illustrating the formation of crystalline SiC in (a) H and (b) A1 samples (phase boundaries are indicated with dashed lines) and (c) the formation of turbostratic graphite in A2 samples annealed at 1400 °C. The orientation of graphene sheets is indicated with guidelines.

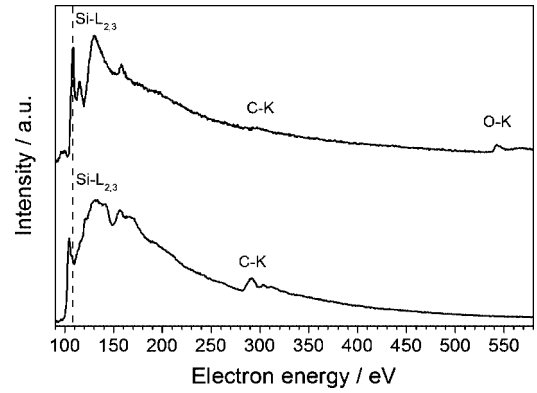

Figure 6. EEL spectra of H 1400 °C samples: amorphous bulk (above) and nanocrystalline SiC regions (below).

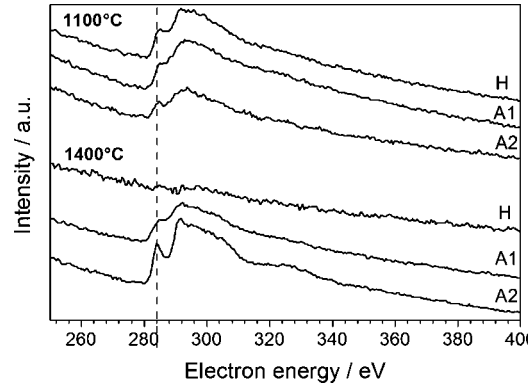

Figure 7. EEL spectra presenting the C−K edge for H, A1, and A2 samples, treated at 1100 °C (top) and 1400 °C (bottom).

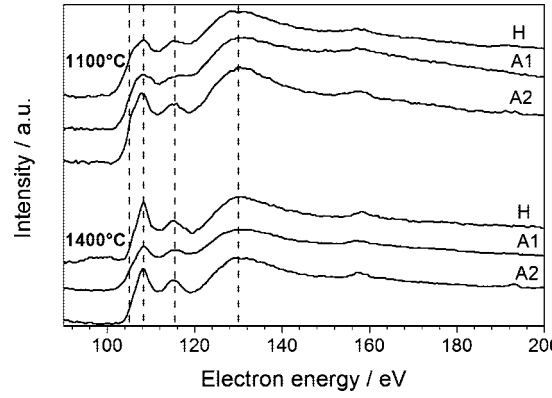

Figure 8. EEL spectra presenting the Si−$L_{2,3}$ edge for H, A1, and A2 samples treated at 1100 °C (top) and 1400 °C (bottom).

distinct shift to higher energies (Figure 9), indicating an increased amount of oxidic bonding in the nearest coordination sphere of silicon. The analysis of boron ELNES features was not possible because of overlapping of the B−K edge with the intense tail of the Si−L_1 edge.

3.3. Oxygen-Dependent Stabilities of the Different Ceramics. The observed different stabilities of the three series of Si−B−C−O ceramics against the component segregation as well as the observed different SiC formation rates at high temperature may be explained by the different oxygen contents in the precursors resulting from the corresponding cross-linking routes: In the case of hydrolysis of the chlorosilane B (H route), only one oxygen atom is introduced as a bridge between two silicon atoms:

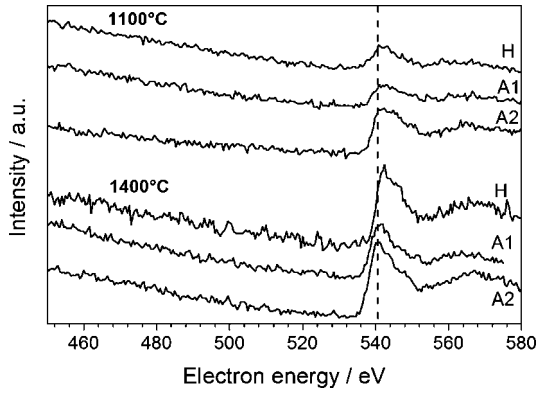

Figure 9. EEL spectra presenting the O−K edge for H, A1, and A2 samples treated at 1100 °C (top) and 1400 °C (bottom).

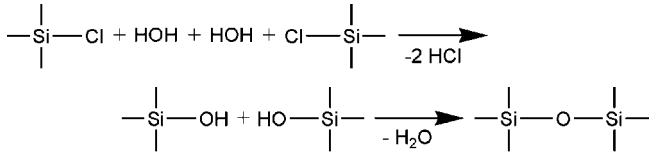

In contrast, during alcoholysis (A1, A2 routes) the whole alkoxy group with at least two oxygen atoms is introduced as a bridging unit:

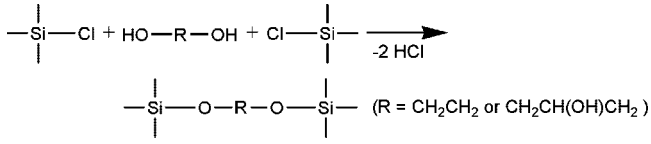

Thus, at least a two times higher amount of bound oxygen is provided in the stoichiometrically substituted chlorosilanes. The results of elemental analysis of the polymer precursors and the resulting SiBCO ceramics from different series support this conclusion: In particular, samples A1 cross-linked with the polyvalent alcohol glycerine showed indeed the highest oxygen content (Table 2), while the lowest oxygen content was found in samples H (cross-linking with water).

The evident influence of the oxygen content in the polymer on the segregation of SiC in SiCO ceramics has been previously reported by Kaneko et al.:[32] With higher oxygen content the Si−C−O ceramics tend to keep the amorphous state. In general, this tendency has been confirmed by our results. However, in some cases, another important factor, the local structural features of polymer precursor, resulting from different bridging units in cross-linking, was found to influence this tendency significantly. For instance, the ceramics of series A1, with the highest final oxygen content (42.7 mol %), still showed a few inclusions of nanocrystalline SiC in the amorphous matrix, in contrast to ceramics of series A2, having no SiC inclusions at all (26.9 mol % of final oxygen).

The different rate of oxygen elimination from the initial precursor during thermal decomposition (Table 2) may also account for specific structural features of polymers from different cross-linking routes (e.g., different amounts of Si-bound and C-bound oxygen in the structure). The exact determination of polymer structure and the related thermal decomposition mechanism are, however, out of the scope of this work.

It is interesting to compare the change of carbon content in the samples of different series. The initial values are 57.7, 59.0, and 56.4 mol % for H, A1, and A2 series, respectively. After ceramization, 45.5, 26.8, and 45.1 mol % of carbon have been found for the individual samples. One can see that though starting with the similar carbon content in different polymers, the elimination rate of carbon may be quite different, depending on the cross-linking route of the polymer precursor. Even by similar content of carbon in the ceramic samples (H and A2 series; 45.5 and 45.1 mol % of final carbon), the distribution of this carbon in the sample is different, again reflecting the influence of the cross-linking route for polymer precursor: in the ceramic sample H the carbon is mainly concentrated in the regions comprised of nanocrystalline SiC inclusions, while a low amount of carbon is detected in the amorphous matrix. In opposite, the same amount of carbon (by approximately the same content of oxygen; see above) is uniformly distributed in the ceramic sample A2, showing no SiC inclusions, but some inclusions of turbostratic graphite instead.

The intentional design of the cross-linking route to control the amount of the oxygen content in the polymer precursor and the specific local structure of polymer allows, thus, to influence the homogeneity of the component distribution and the formation of crystalline phases in the resulting Si−B−C−O ceramic powders up to 1400 °C.

4. Conclusions

Three different polymers were synthesized by hydrolysis and alcoholysis of a boron-containing monomer, namely, tris(1-(dichloro(methyl)silyl)ethyl)borane. Subsequent pyrolysis of the polymers between room temperature and 1100 °C yielded amorphous Si−B−C−O ceramics. Thermal gravimetric analysis (TGA) coupled with in situ mass spectrometry showed that the mass loss is mainly due to outgassing of H_2, CH_4, and C_2H_4 for all the polymers derived from hydrolysis and alcoholysis reaction. Those polymers obtained by cross-linking with the polyvalent alcohols glycerine and glycol showed additional volatile $C_xH_yO_z$ species evolved during pyrolysis resulting in high mass loss up to 75 wt % while the mass loss for the sample cross-linked with H_2O amounts to 35 wt %. Thus, for technical applications, the degree of cross-linking has to be optimized for the alcoholized products to increase the ceramic yield after thermolysis of the Si−B−C−O-polymer. No weight loss was detected for all samples during annealing between 800 and 1400 °C, which is observed when phase segregation in the amorphous silicon oxycarbide takes place without carbothermal reduction of silica.[30] The analyzed thermal decomposition and crystallization behavior of the three polymers revealed a clear correlation with the applied cross-linking route.

The microstructure of the ceramic samples was investigated by analytical electron microscopy (SEM, TEM, and EELS). The polymers obtained by hydrolysis of tris(1-(dichloro(methyl)silyl)ethyl)borane (H series) showed a high tendency to crystallization at 1400 °C in comparison to the

(32) Kaneko, K.; Kakimoto, K. I. *J. Non-Cryst. Solids* **2000**, *270* (1−3), 181–190.

polymers derived from alcoholysis (A1 and A2 series). While the formation of nanosized crystalline SiC particles in the H series samples could be observed, the A1 and A2 samples remained essentially amorphous. The different crystallization features were related to the oxygen content of the polymer-derived Si−B−C−O ceramics. Accordingly, a lower amount of oxygen in the hydrolyzed polymer H leads to a pronounced formation of crystalline SiC phase, while the enhanced oxygen content in the alcoholized polymers A1 and A2 obviously stabilizes the amorphous Si−B−C−O network at temperatures up to 1400 °C. The synthesized Si−B−C−O ceramics withstand decomposition up to 1400 °C and are, therefore, candidate materials for high temperature applications such as ceramic fibers, coatings, and CMCs.

Acknowledgment. This work was financially supported by the German Science Foundation (DFG, Bonn, Germany) under Grants WO 482/11-2, RI 510/36-2, and MU 1166/12-1 as well as by the Fonds der Chemischen Industrie, Frankfurt, Germany. The authors are grateful to Dr. A. Berger for his support in the SEM measurements.

CM701916G